

Nanotechnology-Enabled PCR with Tunable Energy Dynamics

Published as part of JACS Au special issue "Biocatalysis in Asia and Pacific".

Xinmin Zhao, Hongzhen Peng, Jun Hu, Lihua Wang,* and Feng Zhang*



Cite This: JACS Au 2024, 4, 3370–3382



Read Online

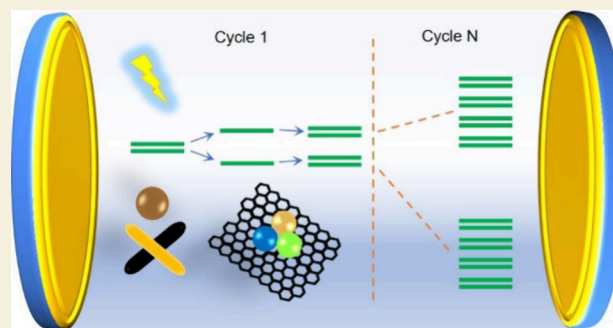
ACCESS |

Metrics & More

Article Recommendations

ABSTRACT: This Perspective elucidates the transformative impacts of advanced nanotechnology and dynamic energy systems on the polymer chain reaction (PCR), a cornerstone technique in biomedical research and diagnostic applications. Since its invention, the optimization of PCR—specifically its efficiency, specificity, cycling rate, and detection sensitivity—has been a focal point of scientific exploration. Our analysis spans the modulation of PCR from both material and energetic perspectives, emphasizing the intricate interplay between PCR components and externally added entities such as molecules, nanoparticles (NPs), and optical microcavities. We begin with a foundational overview of PCR, detailing the basic principles of PCR modulation through molecular additives to highlight material-level interactions. Then, we delve into how NPs, with their diverse material and surface properties, influence PCR through interface interactions and hydrothermal conduction, drawing parallels to molecular behaviors. Additionally, this Perspective ventures into the energetic regulation of PCR, examining the roles of electromagnetic radiation and optical resonators. We underscore the advanced capabilities of optical technologies in PCR regulation, characterized by their ultrafast, residue-free, and noninvasive nature, alongside label-free detection methods. Notably, optical resonators present a pioneering approach to control PCR processes even in the absence of light, targeting the often-overlooked water component in PCR. By integrating discussions on photocaging and vibrational strong coupling, this review presents innovative methods for the precise regulation of PCR processes, envisioning a new era of PCR technology that enhances both research and clinical diagnostics. The synergy between nanotechnological enhancements and energy dynamics not only enriches our understanding of PCR but also opens new avenues for developing rapid, accurate, and efficient PCR systems. We hope that this Perspective will inspire further innovations in PCR technology and guide the development of next-generation clinical detection instruments.

KEYWORDS: PCR, nanoparticle, interface interaction, thermal conductivity, photothermal effect, photocaging, optical resonator, vibrational strong coupling



1. INTRODUCTION

In 1993, Kary Mullis was awarded one-half of the Nobel Prize in Chemistry for his invention of the polymer chain reaction (PCR) method,¹ just under a decade after he independently filed the related invention patent in 1985² and contributed to a *Science* article published the same year.³ Such a short timeline underscores his significant contributions to the development of DNA chemical methods. Originally named by Mullis as “Process for amplifying nucleic acid sequences” in his patent,² PCR fundamentally is a technique for replicating DNA without cells. Its basic principle involves the use of DNA polymerase to rapidly amplify target DNA sequences through a cyclic replication reaction at high temperatures. The standard PCR process includes three main steps. The first step is denaturation—where double-stranded DNA (dsDNA) is heated to 94–98 °C, separating into two single strands (ssDNA); thus, this process is also referred to DNA melting,

with the temperature at which half of dsDNA molecules melts termed the melting temperature (T_m). The second step is annealing—lowering the temperature to 50–65 °C allows primers to bind (hybridize) with the complementary sequences of the target DNA. The third step is extension—raising the temperature to 72 °C, where the DNA polymerase initiates the synthesis of new DNA strands starting from the bound primers. This three-step process is repeated over multiple cycles, each of which doubles the quantity of the target DNA sequence (also termed amplicon), finally leading to an

Received: June 30, 2024
Revised: August 8, 2024
Accepted: August 8, 2024
Published: August 30, 2024



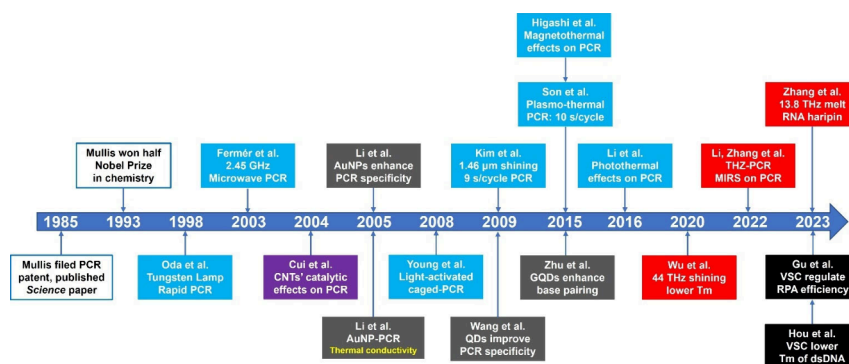


Figure 1. Evolution timeline of innovative/notable advancements in PCR technology. Over the span of nearly four decades, the advancements included in the boxes could be classified into six categories: (a) NP-mediated interface effects (light black colored), (b) catalytic effects (purple colored), (c) NP-mediated thermal conduction effects (e.g., yellow colored text), (d) electromagnetic wave/light-mediated photo/magneto/plasmo-thermal effects (navy blue colored), (e) nucleic acid-based resonant absorption effects (red colored), and (f) water-based resonant coupling effects (dark black colored). Among them, categories (a–c) are associated with matter level effects, while categories (d–f) are related to energy level effects. To highlight significant studies and their contributions to the field, each box contains the name of the lead author(s) and a brief description of their contribution.

exponential increase in the amount of the target DNA fragment.

Currently, various PCR techniques have been developed to meet different application requirements, such as qPCR for real-time quantitative detection,⁴ multiplex PCR that can produce multiple target sequences,⁵ hot-start PCR to significantly enhance specificity,⁶ error-prone PCR for efficiently inserting random mutations,⁷ and isothermal PCR that operates at a constant temperature.⁸ For their basic principles, one can refer to the review article by Nazir et al.⁹ These PCR technologies have been widely applied to the fields of biomedical research and on-site testing,^{10–12} including food safety,¹³ medical diagnosis,^{14–16} and forensic identification¹⁷ among others.

In certain special scenarios, conventional PCR could produce nonspecific products, which significantly reduces amplification efficiency. For instance, cases in forensic identification often involve extremely low template concentrations, making specificity a critical factor in determining the results. To address this issue, scientists have discovered that adding certain substances can significantly improve both the efficiency and specificity of PCR. These additives are usually thought to interact with components of the PCR, such as the templates, primers, polymerases, deoxyribonucleoside triphosphates (dNTPs), and magnesium ions (Mg^{2+}), or simultaneously interact with more than one component, causing changes in the concentration or activity of certain components and thereby altering PCR performance.

From the molecular perspective, additive-based methods to enhance PCR performance can be considered from the following aspects.

- (1) Enriching and locally increasing the concentration of PCR components to enhance efficiency and specificity, such as polyamidoamine (PAMAM) dendrimers and their derivatives, which improve the specificity and efficiency of error-prone and nonspecific PCRs. The optimal concentration is determined by the density of terminal amino groups, and the best concentration of polycationic dendrimers can be 4 orders of magnitude lower than that of fully acetylated and carboxyl-modified dendrimers.¹⁸
- (2) Protecting the activity and thermal stability of polymerases using additives through preferentially

interacting with water molecules, creating an exclusion zone around the polymerases that help to stabilize the water shell surrounding the enzyme, e.g., glycerol,¹⁹ proline,²⁰ sucrose,²¹ and trehalose.²²

- (3) Stabilizing the DNA template, particularly GC-rich DNA templates: to prevent the formation of secondary structures. Substances such as dimethyl sulfoxide (DMSO, competitively accepts hydrogen bonds, allowing the DNA to adopt a more open conformation),²³ betaine (creating crowding effect, essentially promotes a more open and linear template conformation of DNA),²⁴ 7-deaza-dGTP (partially substitutes for dGTP, deoxyguanosine triphosphate, reducing the number of hydrogen bonds),²⁵ and surfactants (interacting with both the DNA and water molecules, potentially affecting the overall conformation)²⁶ are used for this purpose. Conversely, allowing some DNA templates to form secondary structures can selectively amplify DNA sequences. Cations of different types and valences prefer to aggregate a longer ssDNA than a shorter one, achieving selective amplification by filtering DNA fragments of different lengths.^{27,28}
- (4) Increasing specificity by reducing primer dimerization and the T_m of template dsDNA using substances like formamide (acting as a denaturant, weakens hydrogen bonds),²⁹ proline (could disfavor primer–primer interactions by influencing the water molecules around the primers),²⁰ trehalose (influencing water dynamics), and tetramethylammonium chloride (TMAC, by reducing the electrostatic interactions).²²
- (5) Increasing both specificity and efficiency by enhancing the correct hybridization of primers to the template at the annealing phase, e.g., tetraalkylammonium (TAA) derivatives, while inhibiting the binding of dye components (such as SYBR Green I, SGI) to primers in qPCR.^{30,31}
- (6) Increasing PCR specificity by nonspecific binding and stabilization of ssDNA using single-stranded binding (SSB) proteins.²²
- (7) Improving PCR efficiency by eliminating inhibitors present in samples, such as bovine serum albumin (BSA).³²

The emergence of nanotechnology in the late 20th century inevitably led to the integration of nanoparticles (NPs) into PCR research, due in part to their molecular-like properties.^{33,34} On the other hand, the unique attributes of NPs, such as thermal conductivity, photo-/magneto-/plasma-thermal effects, superparamagnetism, and dielectric constant, which dramatically differ from organic molecules, become the key reasons for incorporating NPs into PCR. It is worth noting that when discussing the impact of thermal conductivity on PCR, we specifically refer to thermocycling PCR because precise temperature control significantly affects the specificity of PCR. Several articles have reviewed the impact of NPs on PCR from the perspectives of material properties and regulation mechanisms.^{35–38} However, the regulation of PCR has already transcended the realm of materials alone, since energy-based methods have been found to successfully tune PCR performance, for example: resonant absorption method (e.g., middle infrared stimulation, MIRS) through external laser irradiation and resonant coupling method (e.g., vibrational strong coupling, VSC) through optical resonators even in the dark. Given the development of new mechanisms in recent years, we will revisit the methods of regulating PCR from both material and energy perspectives, hopefully to introduce innovations from different aspects (Figure 1).

2. INTERFACE INTERACTION

In 2005, Li and colleagues reported the remarkable effect of gold NPs (AuNPs) in significantly enhancing the specificity and yield of PCR using a two-round error-prone PCR system. They explained that the enhancement effect of AuNPs was similar to that of SSB proteins—whose affinity to ssDNA is stronger than to dsDNA, which helps to reduce base mismatching and thus lowers the probability of nonspecific amplification.³⁹ Subsequent research by Pan et al. further confirmed that the enhancement effect of AuNPs can be sustained for up to seven rounds of error-prone PCR.⁴⁰ Nevertheless, Vu and colleagues argued that AuNPs do not enhance PCR specificity but rather suppress the amplification of longer amplicons/products while favoring the amplification of shorter amplicons/products,⁴¹ a mechanism similar to the selective amplification of shorter target DNA sequences achieved by metal ions.^{27,28} The nonspecific binding of PCR components by NPs has been a primary focus in explaining these phenomena, with both Vu⁴¹ and Mi⁴² designing rigorous control experiments that independently confirmed that NPs can nonspecifically bind to polymerases, thereby reducing the effective concentration of the polymerase in PCR.

Mandal et al. also systematically studied the affinity between AuNPs and PCR components, finding that the affinity of AuNPs to polymerases was much larger than that between AuNPs and primers or template DNA. When AuNPs bind to polymerases, they can increase the thermal denaturation temperature of the polymerases by 8 °C (from 73 to 81 °C), indicating that AuNPs can enhance the thermal stability of polymerases.⁴³ Atomic force microscopy (AFM) could visualize the interactions between AuNPs and polymerases⁴³ as well as DNA templates.⁴⁴ From this perspective, modifying the surface properties of NPs should eliminate this interfacial effect, and increasing the polymerase concentration or adding BSA as a competitive agent can also reverse this effect. This is consistent with the findings of Wan et al., who reported that equal total surface area is required to reach a same inhibition

effect, i.e., larger AuNPs require lower inhibitory concentrations, strongly supporting the interface interaction theory.⁴⁵

Due to the positive effects in foundational research, NP-PCR systems have quickly been validated in various application scenarios. For example, Yang et al. used AuNPs to enhance simultaneous overlap extension PCR (SOE-PCR), significantly improving the sensitivity and yield of SOE-PCR by optimizing the concentrations of both polymerases and AuNPs, successfully fusing six λ DNA fragments in one reaction.⁴⁶ El-Husseini et al. successfully applied AuNP-PCR to improve the sensitivity and specificity of virus detection.⁴⁷ Ye et al. utilized the electrostatic interaction between AuNPs and primers with polymerases to achieve a hot-start effect in the LAMP system, successfully applying it to clinical detection of rotavirus, reducing the false-positive rate from 76% to 0% and lowering the detection limit to 1000 copies/mL, meeting the needs for rapid clinical diagnosis.⁴⁸ However, there are also reports of negative effects; for example, Haber et al. reported that AuNPs can quench the fluorescence of the dye SGI, altering the amplification spectrum of qPCR, leading to erroneous results, and also destabilizing the products. Moreover, they found no evidence for AuNPs enhancing thermal conductivity or any enhancement effects on PCR,⁴⁹ apparently challenging all of the above findings.

It was found that AuNPs as the core of dendrimers can help maintain their three-dimensional structure, which increases their interaction area with PCR components. Regarding the optimal concentration for enhancing PCR efficiency and specificity, the core-shell structure requires 3 orders of magnitude lower concentration compared to dendrimers alone and 1 order of magnitude lower than AuNPs alone. This clearly demonstrates that the enhancement effect of NPs on PCR is achieved through the interface interaction.^{50,51} Yuan et al. studied the impact of surface charge on PCR by comparing poly(diallyl dimethylammonium) (PDDA) coated AuNPs with citrate-coated AuNPs, finding that a positively charged surface required 3 orders of magnitude lower concentration of AuNPs than a negatively charged surface, further illustrating the contribution of surface charge to interface interaction theory.⁵²

Due to the significant enhancement effect of AuNPs in PCR, logically, other NPs such as carbon nanopowder (CNP), upconversion NPs (UCNPs), quantum dots (QDs) including graphene quantum dots (GQDs), carbon nanotubes (CNTs) and (oxidized) graphene (GO), magnesium oxide NPs (MgO NPs), magnetic NPs (MNPs), metal-organic frameworks (MOFs), and their composites might also impact PCR. The interface interaction theory could also account for their effects on PCR (Figure 2). For example, Zhang et al. found that CNP can enhance repeated and long PCR by binding with DNA.⁵³ Wang et al. reported for the first time that QDs can improve the specificity of PCR under different annealing temperatures and DNA template lengths (multiplex PCR), although not enhancing the PCR efficiency. The authors proposed that the interaction between polymerase and QDs could partially inhibit the activity of the polymerase.⁵⁴ Ma et al. reported that QDs modified with mercaptoacetic acid (MAA) or streptavidin (SA) significantly improved the PCR yield and specificity. The authors claimed that the observed effect was not due to the surface property of QDs but instead due to the QD itself, apparently throwing out a confusing conclusion.⁵⁵ Liang et al. found that the right concentration of QDs can enhance the specificity of multiplex PCR, but excessive QDs

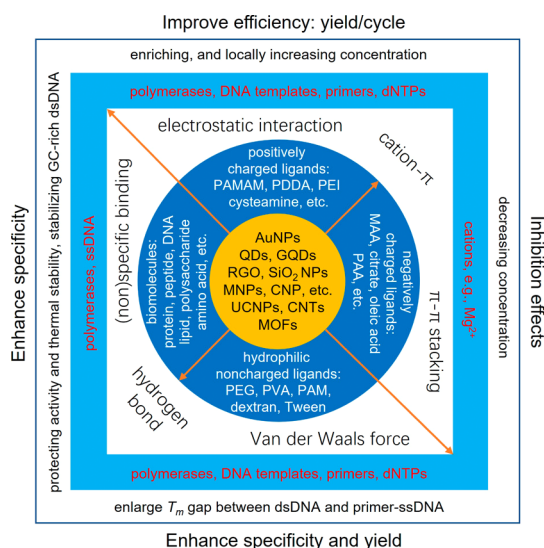


Figure 2. Effects of interface interaction of NPs on PCR. This diagram categorizes various interactions and their mechanisms for influencing PCR specificity and efficiency. Complex interactions between main PCR components, e.g., polymerases, DNA templates, primers, dNTPs, and Mg^{2+} , and a range of ligand molecule-coated NPs can modulate the specificity and efficiency of PCR. From inner to outer, the first circle refers to the core materials of NPs, the second circle has been separated into quadrants for ligands with different properties wrapping around NPs, the third framework includes different interactions between ligands and NPs, the fourth framework involves the main PCR components, polymerases, DNA templates, primers, Mg^{2+} , and dNTPs, and the fifth framework points out the mechanisms by which NPs can influence PCR. Each category is critical for understanding how NPs should be designed to optimize PCR efficiency and specificity. The diagram, organized by the adjacency principle, aligns related molecular interactions and compounds around the central components of PCR—polymerases, DNA templates, primers, and dNTPs. Each quadrant adjacent to these key elements illustrates a different category of interactions or molecules that can influence the PCR process. The blue colors also indicate the interaction with water, e.g., hydration, and the orange-colored arrows represent the contribution of ligands to the diameter of NPs and the radius of interface interaction. With the adjacency rule, the components, interactions, and mechanisms in the same framework can combine together for the synergistic effects, which even fit for the effects outside the frameworks.

showed an inhibitory effect, which can be reversed by increasing polymerase concentration or adding BSA.⁵⁶ Sang et al. first used the interface interaction between QDs and polymerases to achieve a hot-start effect in PCR⁵⁷ and later found that this binding can partially inhibit the activity of polymerases during thermal cycling, thereby effectively enhancing the specificity of qPCR.⁵⁸ Hwang et al. reported that the enhancement effect of UCNPs on PCR specificity was related to their concentration and particle size, again suggesting the mechanism based on interface interaction theory.⁵⁹

Some carbon-based composite materials have also been applied to regulate PCR, such as polydopamine and its carbonized coating on SiO_2 NPs, which can regulate PCR efficiency through interactions with polymerases and primers.⁶⁰ Cao et al. used polyethylenimine (PEI) modified multiwalled carbon nanotubes (MWCNT/PEI) to improve the specificity and efficiency of PCR. Both positively charged and partially acetylated PEI significantly improved PCR efficiency and

specificity, whereas negatively charged PEI derivatives were ineffective, clearly indicating that electrostatic adsorption also belong to the interface interaction theory.⁶¹ Yüce et al. compared the effects of three differently charged CNTs on PCR, finding that only CNTs with Tween-20 (surface is rich in OH groups) and amino-functionalized CNTs enhanced PCR, whereas carboxylated CNTs inhibited PCR, illustrating the molecular mechanism of PCR modulation by surface groups—negative surfaces not only fail to bind primers and template DNA but also reduce Mg^{2+} concentration, producing the inhibitory effect.⁶² GO⁶³ and GQDs have both been used to enhance PCR, though their mechanisms differ: Zhu et al. found that GQDs can both π - π stack with primers and electrostatically bind Mg^{2+} , enhancing both base pairing efficiency between primers and templates and the polymerase activity.⁶⁴ Based on the separate enhancing principles of AuNPs and GO, Jeong et al. reported that synthesized Au/GO composites were 1.3–2.4 times more effective than only using AuNPs or GO alone.⁶⁵

The stability of NPs in solution is usually achieved through surface ligand charges, typically negative, e.g., citric or oleic acid. The general mechanism for these negatively charged NPs enhancing PCR specificity and efficiency is believed to involve their surface affinity for dsDNA and ssDNA, with a preference for binding ssDNA; this phenomenon is due to two reasons. First, dsDNA has a higher negative charge density than ssDNA, so dsDNA exhibits a larger repulsive force against negatively charged NPs than ssDNA. Second, the rigidity of dsDNA compared to ssDNA makes it less conducive to wrapping around NPs. This explanation is similar to the action mechanism of SSB proteins and, therefore, is widely used to explain the enhancement effect of NPs on PCR.^{39,54} Third, the enhancement effect of NPs on PCR through their surface properties (even including surface area) is related to the particle size—because the surface area of NPs in contact with the outside world is directly proportional to the square of the NP radius. It was reported when detecting *Staphylococcus aureus* and *Salmonella enteritidis*, MNPs with an average particle size of 1 μm enhanced PCR efficiency, while 60 nm MNPs had no enhancement effect; the authors claimed that MNPs enhance PCR specificity and sensitivity through a surface enrichment effect.⁶⁶

MNPs possess unique properties such as magnetically controlled movement and magnetothermal conversion, offering specific effects in PCR that are distinct from those of AuNPs, QDs, CNTs, SiO_2 , and others. For example, Higashi and colleagues controlled the rotation of an external magnetic field to stir the MNPs at the nanoscale and found that the PCR yield decreased as the rotational frequency increased (1.0–20 Hz).⁶⁷ After removing the external magnetic field, they found that MNPs formed clusters to capture the polymerases, thereby inhibiting PCR by reducing the number of active polymerases during the thermal cycling.⁶⁸ By exploring the selective binding to ssDNA and the ability to immobilize polymerase, Sun and colleagues brought the recently popular nanocomposite material, metal–organic frameworks (MOFs), into this field, finding that two types of MOF materials (UiO-66, ZIF-8) can also enhance the sensitivity and efficiency of PCR.⁶⁹ Other NPs, such as functionalized tetrapodal ZnO nanostructures,⁷⁰ MgO NPs,⁷¹ hexagonal boron nitride (hBN) NPs,⁷² and ZnO nanoflowers,⁷³ have similarly been documented for their abilities to enhance PCR and pathogen detection and will not be elaborated further in this Perspective.

3. HYDROTHERMAL CONDUCTION

As the DNA replication process requires the dsDNA to be melted before primers can bind to the template ssDNA, the heating and cooling of the entire system are closely related to the thermal conductivity of the PCR solution. Interestingly, the same year when Li et al. published the first paper on AuNPs-PCR in *Angewandte Chemie International Edition*,³⁹ a research group from National Cheng Kung University in Taiwan reported very similar results in *Nucleic Acids Research*. Unlike the SSB protein binding ssDNA theory, they for the first time proposed that AuNPs change the thermal conductivity of the PCR solution.⁷⁴ However, in 2008, Vu et al. eliminated such an effect on PCR by coating the AuNPs with a self-assembled monolayer (SAM) of hexadecanethiol, providing strong evidence against the thermal conduction theory.⁴¹ Following this, discussions about the impact of NP-based thermal conduction on PCR have become a hot topic. In 2008, Zhang and colleagues used CNTs, whose thermal conductivity could be 1 order of magnitude higher than that of AuNPs (MWCNTs, 3000 W/mK; SWCNTs, 6000 W/mK),⁷⁵ and discussed in detail the effects of CNTs on PCR. They concluded that the addition of CNTs enhanced the thermal conductivity of a solution, facilitating rapid thermal equilibrium and convective heat transfer in PCR, thus promoting specific annealing of primers and templates and reducing the probability of nonspecific or smearing/tailing products.⁷⁶

Due to the fact that TiO₂ NPs in aqueous solution can increase the thermal conductivity by 33% with just a 5% volumetric ratio,⁷⁷ in 2010, Abdul Khaliq et al. used the high thermal conductivity of TiO₂ NPs to achieve a significant increase in PCR efficiency: the yield increased up to 7 times, and the total reaction time was reduced by 50%. The authors also validated the faster heat transfer of reaction buffer with TiO₂ NPs using a numerical simulation (fluent K epsilon turbulent model).⁷⁸ Abdul Khaliq et al. enhanced the thermal conductivity of the PCR solution using graphene nanoplates (GNFs), experimentally reducing the number of PCR cycles by up to 65%, a finding also validated in numerical simulation experiments.⁷⁹ Lin et al. found that AuNPs could enhance the melting efficiency of dsDNA—including the dissociation between mismatched primers and DNA templates, further confirming the theory that AuNPs enhance PCR through hydrothermal conduction.⁸⁰ Madadelahi et al. found that the high thermal conductivity of diamond NPs also can increase PCR efficiency by up to 5 times and shorten PCR time by at least 40%.⁸¹

4. SYNERGETIC AND CATALYTIC EFFECTS

The discussion above highlights the ongoing debate between the interface interaction theory and hydrothermal conduction theory. In principle, interactions between NPs and PCR components are inevitable. In traditional heating modes, where water is the primary medium for heat transfer, if NPs bind with PCR components (especially primers and templates), then they will become a direct medium for thermal conduction. Therefore, the actions of interface interaction and thermal conduction could produce synergistic effects. For example, polyethylene glycol-PEI-coated AuNPs (PEG-PEI-AuNPs), because of their capability to offer surface electrostatic interaction and efficient thermal conductivity, greatly enhance the specificity and efficiency of error-prone PCR. This impact is particularly significant in GC-rich PCR systems where

thermal conduction becomes more critical.⁸² Jia and colleagues demonstrated that reduced GO (RGO) selectively binds with Pfu polymerase, leading its zeta potential to increase from -20.3 to 5.39 mV. This shift enhances the interaction between negatively charged primers and templates, thereby improving primer annealing and extension, lowering mismatch rates, and boosting PCR specificity. Additionally, due to the exceptionally high thermal conductivity (5300 W/mK) of RGO, the RGO-PCR system can achieve thermal equilibrium more quickly—minimizing the isothermal delay between PCR components and the heating block and ensuring a more consistent temperature distribution throughout the PCR. This confirms the synergistic effect of interface interaction and thermal conduction.⁶³ Additionally, Lou and colleagues found that AuNPs can bind to primers and reduce their dimerization T_m by about 1.0 – 1.7 °C, without altering the T_m between primers and templates. This alteration widens the T_m gap between these two hybrids, thereby improving both the efficiency and specificity of PCR through a synergistic effect.⁸³

Since the interface interaction between NPs and PCR components is inevitable, Jiang et al. systematically studied the interaction sequence of AuNPs and their surface ligands with each component of the loop-mediated isothermal amplification (LAMP) system—such as Mg²⁺, template DNA, dNTPs, primers, and polymerase. They found that first mixing AuNPs with primers can slow the LAMP reaction, while other mixing sequences accelerate it. The acceleration mechanism was explained by the role of AuNPs and their aggregates acting as a structural scaffold similar to proteins, creating a favorable surface environment for the reaction. Thus, the surface ligands of AuNPs are critical; when this surface environment resembles that of proteins, it facilitates the acceleration of LAMP, with ligands like BSA and glutathione (GSH) showing a more pronounced accelerating effect than PEG or polyvinylpyrrolidone (PVP).⁸⁴ As this study utilized an isothermal amplification reaction, it strategically sidestepped the topic of the thermal conductivity of NPs—implying that the enhancement effect of AuNPs on PCR is independent of their own thermal conductivity. However, the authors also reported that to achieve equivalent efficiency, AuNPs can lower the reaction temperature of LAMP by 5 °C (from 55 to 50 °C), reintroducing a twist in the seemingly settled theoretical debate.

It is worth noting that in 2004, Cui et al. reported that single-walled nanotubes (SWNCTs) can significantly enhance PCR efficiency by aggregating reaction components. More importantly, they found that SWNCTs could mimic the role of Mg²⁺ by acting as an electron acceptor and coenzyme in PCR, potentially replacing Mg²⁺ to maintain the catalytic activity of polymerases.⁸⁵ This study was significant for two reasons. First, it demonstrated the catalytic activity of NCTs. Second, it predated Li et al.'s report on AuNP-enhanced PCR by a year.³⁹

5. ELECTROMAGNETIC EFFECTS

5.1. Magnetothermal Effects

Under alternating magnetic fields, MNPs possess a magnetothermal conversion effect and can serve as nanoscale heaters to develop rapid PCR instruments by replacing traditional PCR heating modes, with the alternating magnetic field also acting as a reaction switch.⁸⁶ Although magnetothermal conversion counts as a nontraditional heating mode, it requires the addition of MNPs to the PCR, which introduces other issues in

PCR, e.g., high concentration-induced inhibition effects and quantitative detection calibration, and therefore will not be discussed in detail here.

5.2. Photothermal Effects

The principle of photothermal conversion uses the resonant absorption capacity of light-absorbing substances (such as water) to efficiently convert light energy into heat through photoacoustic coupling. Interestingly, instead of using the magnetothermal effect of MNPs, Li et al. developed a photothermal PCR technique in combination with a pulse near-infrared (NIR) laser (808 nm, 460 mW).⁸⁷ Similarly, Kadu et al. applied the photothermal effects of triangular AuNPs and silver (Ag) NPs to an efficient PCR technique, in which 808 nm laser irradiation can reach a temperature of ~ 90 °C.⁸⁸

Apart from using NPs to improve the thermal conductivity of PCR buffers, the rate of temperature change can also be achieved by altering the heating mode. Initially, Oda et al. replaced traditional contact heat sources with a tungsten filament lamp (Figure 3A), using light and compressed air for rapid heating (10 °C/s) and cooling (20 °C/s), respectively, achieving temperature changes between 94 and 55 °C, reducing the cycle time to 17 s.⁸⁹ It is now known that the light emitted by a tungsten filament lamp is broad-spectrum, and the specific frequencies involved can be measured by spectrometers, which can detect the fingerprint absorption bands of water from the ultraviolet (UV) to the terahertz range. Using a similar tungsten lamp, Hühmer et al. developed a PCR apparatus that allowed for precise temperature control (Figure 3B), with the heating rate 30 times faster and the cooling rate 15 times faster than traditional contact heating methods. Moreover, by using capillaries, they reduced the reaction volume to subnanoliter levels.⁹⁰ All of these advancements utilized the principle of resonant absorption for photothermal conversion of water.

Given that specific materials have specific absorption frequencies for light, exploring the interaction between specific electromagnetic frequencies and PCR components has become a new direction. For example, Fermér et al. were the first to use focused microwave radiation (2.45 GHz) as a heat source for PCR, reducing the reaction time by half compared to traditional 25-cycle PCR, which takes about 2 h, including a 12 min heat activation phase.⁹³ Five years later, Kim et al. developed a rapid qPCR system (Figure 3C) using low-power (~ 30 mW) NIR lasers (1.46 μm), increasing the cycle rate to 9.25 s/cycle and reducing the reaction volume to nanoliters.⁹¹ They further refined this approach by running qPCR on a culture dish using contact printing technology, creating uniformly sized nL-droplet arrays on a disposable polystyrene dish, and performing qPCR with laser heating, boosting the rate to 9 s/cycle.⁹⁴ Thus, a 25-cycle PCR could be completed in 3.75 min—essentially reaching the speed of colloidal gold testing paper. Six years later, Son et al. used the efficient plasmonic photothermal properties of a gold film (Figure 3D), achieving rapid PCR thermal cycling within 5 min for 30 cycles by using a 450 nm light emitting diode (LED).⁹² Another five years had passed, and Li et al. demonstrated an all-optical qPCR system using fiber optic microcavities and an ultrafast laser heating system. Using a 1.44- μm NIR laser, resonantly absorbed by water, combined with a Fabry–Pérot (FP) interferometer, they achieved nanoscale reaction volumes (down from the traditional 20 μL to 0.2 nL), ultrafast

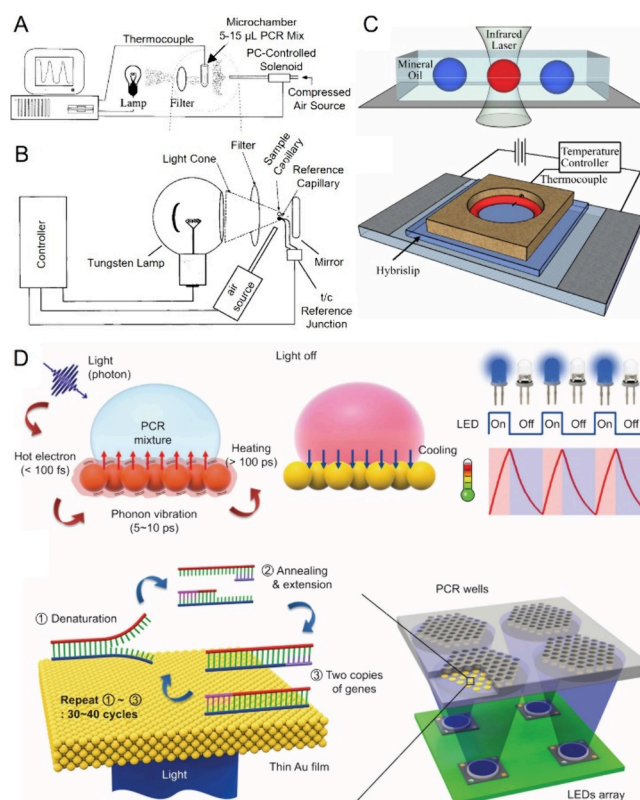


Figure 3. Structural evolution of photothermal PCR devices. (A) Schematic of a PCR device heated by a tungsten filament lamp. This configuration uses a traditional light source, where the tungsten filament lamp provides rapid and uniform heating across the PCR reaction chamber, replacing conventional contact-based heating elements. The lamp heated the reaction mixture directly, enabling fast thermal cycling. Reproduced from ref 89. Copyright 1998, American Chemical Society. (B) Tungsten filament lamp heated capillary nL-volume PCR device. This design incorporates a tungsten filament lamp to heat a capillary tube containing the PCR mixture. The capillary tube helps to minimize the reaction volume to nanoliters, enhancing thermal responsiveness and reducing cycle times due to the smaller thermal mass. Reproduced from ref 90. Copyright 2000, American Chemical Society. (C) NIR laser heated nL-volume qPCR device. This setup uses a 1.46- μm laser to heat the PCR reaction, targeting the absorption bands of water. The laser-focused energy allows for precise and localized heating of a nL-volume reaction, significantly speeding up the PCR process by enhancing the rate of temperature change during the thermal cycling. Reproduced from ref 91. Copyright 2009, Optical Society of America. (D) Blue light LED heated rapid PCR device. Utilizing a 450 nm LED as the heat source, this device leverages the photothermal properties of specific materials (e.g., AuNPs) that efficiently convert light to heat. The use of an LED allows for uniform light distribution and rapid thermal cycling, which are suitable for high-throughput PCR applications that require fast processing times. Reproduced from ref 92. Available under a CC BY license. Copyright 2015 Jun Ho Son et al.

temperature responses (from 30 to 0.45 s), real-time temperature feedback, and label-free quantitative detection. However, due to conservative timing settings, their experiments merely reduced the traditional 90 min duration to 40 min.⁹⁵

5.3. Nonthermal Effects

The research on thermal conduction has primarily focused on the water component in PCR, which has been considered only

as a solvent for thermal conduction so far. In fact, the denaturation step of PCR only requires the conversion of dsDNA into ssDNA, so the most direct method is to find a way to melt dsDNA. To this end, Edwards et al. discovered that microwave irradiation (2.45 GHz) at 109 ± 8 W can cause dsDNA to denature at temperatures much lower than its T_m (from -20 to 20 °C), and this effect is independent of the length of the dsDNA.⁹⁶ This phenomenon could be due to several reasons. First, it is possible that as the number of nucleotides increases, energy is directly transferred to oligonucleotides, allowing dsDNA of different lengths to exhibit the same T_m under the same microwave power. Second, microwave radiation can disrupt the binding of cations to negatively charged DNA, as cations and anions move in opposite directions under the electromagnetic field; therefore, under specific microwave power, the anions of phosphate backbones and cations will completely separate, causing mutual repulsion of the negative charges on the two strands. This makes the double helix unstable, so melting actually minimizes the repulsive potential energy of the negative charges. Finally, regarding the dielectric constant, ssDNA is larger than dsDNA, so when dsDNA begins to melt into ssDNA, the coupling with the electromagnetic field becomes stronger, leading to more energy transfer to overcome the hydrogen bonding within the remaining dsDNA. The authors believe that one or a combination of these possibilities could be the reason why an electromagnetic wave melts ssDNA.⁹⁶

With the advantages of light-driven PCR, theoretical simulations have also begun to focus on the interactions between light and PCR components. In fact, 50 years ago, Frohlich et al. proposed that coherent millimeter wave irradiation at 0.05 THz could affect lots of biological activities based on nonthermal effects of frequency resonance.⁹⁷ Thirty-five years later, Alexandrov et al. calculated that THz light irradiation can cause dynamic melting of dsDNA, meaning that when the intensity and frequency of THz light reach a certain threshold, dsDNA can locally melt (forming bubbles), which was predicted to affect gene replication and transcription processes.⁹⁸ After another 10 years, Wu et al. calculated that purine bases can resonantly adsorb a 44-THz wave, thus breaking their connecting hydrogen bonds (Figure 4A). This can increase the average rate of dsDNA unwinding by 20 times, thus greatly reduce the T_m (Figure 4B).⁹⁹ Zhang et al. utilized 53-THz light that can be absorbed by the carbonyl group, causing the carbonyl-connected hydrogen bonds to break, thus reducing the T_m of dsDNA (Figure 4C).¹⁰⁰ Li et al. within the same research group further validated the advantages of 53-THz light in improving the PCR performance. The experimental results showed that the T_m of dsDNA decreased by at least 3 °C, and the melting time was reduced by 80% (Figure 4D).¹⁰¹ With the help of molecular simulation, Zhang et al. recently reported that 13.8-THz irradiation can promote the melting of RNA hairpins (Figure 4E).¹⁰² These findings have laid both theoretical and experimental foundations for the development of low-temperature, rapid PCR.

5.4. Photochemical Regulation

There is another photochemical approach for regulating PCR known as “photocaging”,¹⁰³ where irradiation with light of a specific wavelength can remove the caging group—preventing its linked nucleosides from being recognized by DNA polymerase. Based on this principle, Young et al. attached a

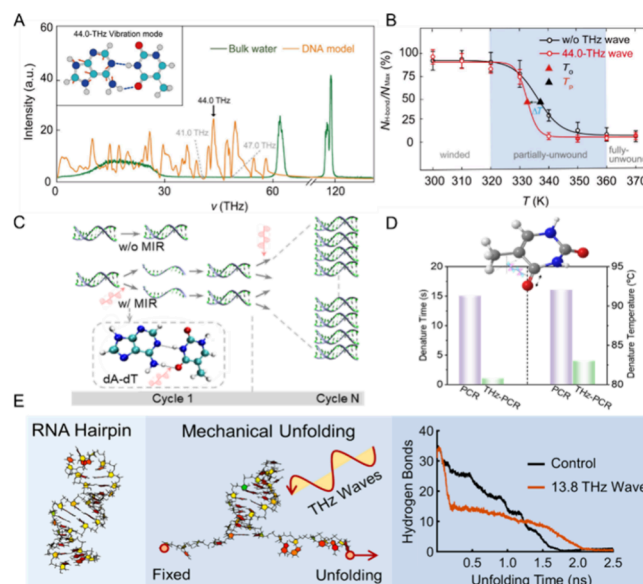


Figure 4. Melting nucleic acids with the THz light of specific frequencies. (A) Molecular simulation of the vibrational frequencies of bulk water and a DNA model. Compared with the vibrational frequencies of both water and DNA molecules, one could select an appropriate THz frequency for studying resonant absorption and coupling. Reproduced from ref 99. Copyright 2020, American Chemical Society. (B) Simulation results for accelerating dsDNA unwinding with 44-THz light. The THz illumination can enhance the melting of dsDNA by disrupting hydrogen bonds at a faster rate compared to conventional heating methods. Reproduced from ref 99. Copyright 2020, American Chemical Society. (C) Schematic of THz light-assisted PCR. THz light can be integrated into the PCR process to improve the efficiency of thermal cycling and enhance the denaturation phase by selectively exciting specific vibrational modes in the DNA molecule. Reproduced from ref 100. Copyright 2023, American Chemical Society. (D) Experimental results of DNA melting facilitated by 53-THz light resonantly absorbed by carbonyl groups. Experimental data show that 53-THz light, which resonates with the carbonyl group, can accelerate DNA melting and lower the T_m . This effect is due to the disruption of the hydrogen bonds linked to the carbonyl groups in the DNA backbone. Reproduced from ref 101. Copyright 2023, American Chemical Society. (E) Simulation design and results for RNA hairpin melting promoted by 13.8-THz light. The simulation data illustrate how THz light can facilitate the melting of RNA hairpins. The schematic shows the simulation setup where THz light targets specific vibrational modes in RNA, promoting the unfolding of the hairpin structure. Reproduced from ref 102. Available under a CC-BY-NC-ND license. Copyright 2023 Qin Zhang et al.

caging group, 6-nitropiperonyloxymethyl (NPOM),¹⁰⁴ to the heterocyclic base of thymidine nucleotide of primers (Figure 5A). UV light (365 nm) shining can cleave NPOM, thereby enabling control over the initiation of PCR at any stage¹⁰⁵ (Figure 5B–D). One year later, they confirmed that most polymerases cannot recognize and read through an NPOM-modified DNA template, thus successfully developing a light-activated PCR method for inducing DNA mutations.¹⁰⁶ In the same research group, Chou et al. simplified the NPOM group to an *o*-nitrobenzyl (ONB) caging group, which they attached to the tyrosine residue (Y671) of the polymerase, thereby blocking the activity of enzymes—occupying the site that normally binds with dNTPs. Then, the ONB group can be removed by 365 nm UV illumination, restoring the wild-type polymerase—enzyme activity recovers, which achieved

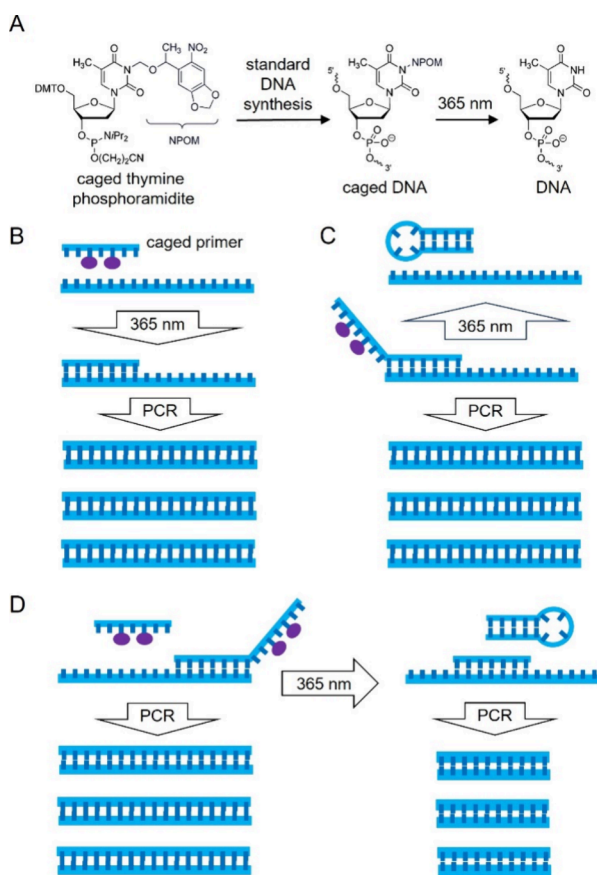


Figure 5. Light-activated PCR. (A) Synthesis of caged-ssDNA using the caging group NPOM. NPOM is covalently linked to a nucleoside to create caged DNA. UV light exposure cleaves the NPOM group, releasing the active DNA for use in amplification. Reproduced from ref 106. Available under a CC-BY-NC license. Copyright 2009 Douglas D Young et al. (B–D) Different strategies for light-activated PCR using caged primers. These panels depict various methodologies employing caged primers to initiate PCR selectively. This can involve controlling the start time of amplification (B), pausing the reaction (C), or selectively activating different parts of a complex DNA template under light control (D). Each strategy uses UV light to remove the caging group at specific stages, thus permitting a tailored approach to PCR amplification based on light exposure.

temporal control over polymerase activity through light-activated PCR.¹⁰⁷

The ability to control PCR initiation with light opens doors for techniques like mutagenesis. By strategically targeting specific primers with photocaging groups, researchers can introduce precise mutations into DNA sequences for functional studies. On the contrary, by controlling the timing of light exposure to cleave the caging group on primers, researchers can initiate amplification only for the targeted sequence. This could be particularly valuable in cancer diagnostics, where identifying specific mutations within a background of healthy DNA is crucial. Moreover, photocaging can be integrated into biosensing platforms, where specific DNA sequences trigger a light-activated PCR reaction. This could be used to develop point-of-care diagnostic tests with high sensitivity and specificity.

5.5. Vibrational Strong Coupling

Previous efforts on regulating PCR focused not only on temperature manipulation but also primarily on controlling

nonwater components in PCR, no matter the theories, i.e., interface interaction, thermal conduction, and even catalytic effects. Interestingly, few studies have really targeted water molecules in PCR as a main component for regulation, except for hydrothermal and photothermal methods that only use water as the medium for transferring heat but not reactants. However, two inspiring studies claimed that PCR efficiency can be regulated by optical microcavities.^{108,109} They experimentally employed an AuNP solution as dynamic optical microcavities, varied “cavity lengths” by NP concentrations, and amplified the read-out signal with the qPCR efficiency. Based on their understanding of quantum biology, the authors proposed that the NP concentration-dependent oscillation of PCR efficiency can be ascribed to the biophotons, which drives DNA replication, whereby they further employed density function theory (DFT) and calculated that these biophotons must be released by dNTPs, and the frequencies were determined to be 34.2 THz,¹⁰⁸ 33 THz, and 84 THz¹⁰⁹ in two separate articles. In fact, the kinetics of chemical reactions can be experimentally modified within the optical resonators, e.g., FP cavities, even in the dark, suggesting another theory; VSC could well account for the observed phenomena.^{110–113}

Due to the poor optical resonators formed by AuNP solution, it is natural for researchers to make best use of stable optical cavities with high quality factors. To this end, Gu et al. recently reported using VSC (Figure 6A) to regulate the efficiency of isothermal amplification reactions—recombinase polymerase amplification (RPA).¹¹⁴ Because the temperature variation can influence the stability of optical resonators, isothermal amplification of DNA should be an optimized substitution for conventional temperature-changing PCR. As we know, VSC is an amazing effect derived from quantum electrodynamics (QED),¹¹⁵ utilizing resonant coupling of optical cavities and molecules to induce Rabi splitting of the resonance frequency, forming two new polariton energy levels (Figure 6B).¹¹¹ Because the changes in molecular energy levels can significantly impact the chemical reactions they participate in, VSC studies in the field of chemistry have been referred to polariton chemistry as well.^{116,117}

In experiments, by merely adjusting the distance between two mirrors in an optical cavity (Figure 6C), Gu et al. realized the VSC-based modification of RPA efficiency with a maximum inhibition rate of ~42% (Figure 6D). When the cavity mode of an optical resonator, e.g., FP cavity, is tuned to resonate with the frequency of the O–H vibration of water molecules, Rabi splitting of the vibrational energy levels of water can produce two new polariton energy levels. If the difference between the two new energy levels exceeds the half-width of the O–H vibrational absorption peak, it forms a VSC state (Figure 6E). The dependency of RPA efficiency on the cavity length strongly proves the effect of the VSC with the O–H stretching vibration on RPA (Figure 6F). Due to the complexity of PCR reactions, which involve multiple components and multiple simultaneous reactions, currently using the FP cavity with a single vibrational frequency of water molecules for resonant coupling cannot arbitrarily control complex reactions, e.g., PCR. However, we can initially use optical resonators to obtain response frequencies for individual reactions. For example, studies on VSC effects on the hydrolysis reactions of ATP¹¹⁸ and sucrose,¹¹⁹ as well as the melting¹²⁰ and assembly¹²¹ of DNA, have identified resonance frequencies that can regulate these reactions. We believe that combining these single frequencies temporally and spatially to

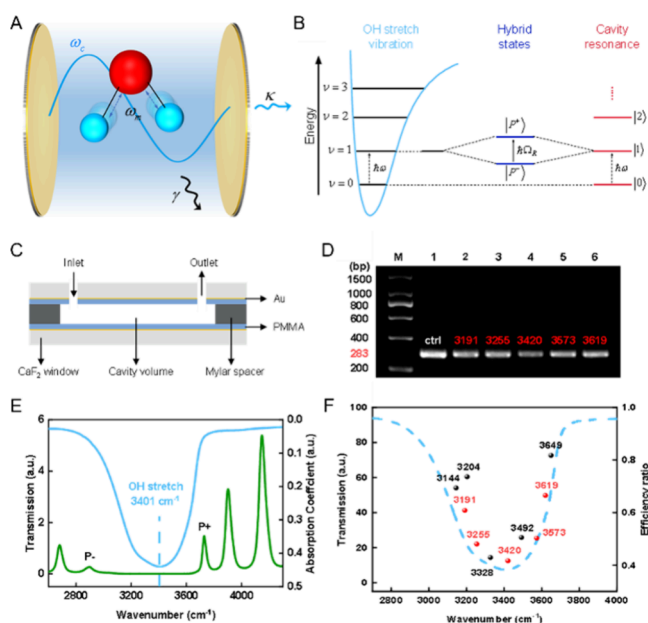


Figure 6. Isothermal DNA amplification within an optical resonator. (A) Schematic of VSC between the optical cavity and water molecules: ω_c , ω_m , κ , and γ represent the cavity mode frequency of the resonator, the vibrational frequency of water molecules, and the dissipation rates of the cavity and molecules, respectively. (B) Rabi splitting of hybrid energy states due to resonance coupling between the O–H stretching vibration and the resonator cavity mode can produce two new polariton energy levels, the upper-level P^+ and the lower-level P^- . (C) Diagram of the optical cavity used as a liquid reaction chamber. This setup highlights how the optical cavity serves to contain the reaction mixture for PCR amplification. (D) Gel electrophoresis showing a comparison of DNA amplification efficiency in liquid pools with different cavity lengths. This panel demonstrates how cavity length (represented by cavity modes in wavenumbers) impacts the efficiency of DNA amplification: the brighter of the gel bands, the greater the efficiency of DNA amplification. (E) Infrared transmission spectrum showing the energy level changes after water molecules undergo VSC with the resonator. This spectrum provides insight into how the interaction between the cavity and water molecules affects the energy landscape of water. (F) Correlation between DNA amplification efficiency and the water transmission spectrum at different cavity lengths. All figures were reproduced from ref 114. Copyright 2023, American Chemical Society.

control complex biological reactions, e.g., synthesis of DNA, protein, might be a future direction for development in chemistry and biomedical science.

Despite the inherent safety advantage of *in vitro* PCR compared with *in vivo* techniques, the development of faster methods based on electromagnetic effects necessitates prioritizing operator safety. Potential hazards include exposure to thermal effects from high-intensity light sources used for rapid heating and the unknown long-term health risks associated with repeated nonthermal radiation exposure. Further research is crucial to ensure a safe working environment for personnel while validating the efficacy of these novel techniques against established protocols.

6. CONCLUSIONS AND OUTLOOK

In conclusion, this comprehensive Perspective delineates the pivotal roles of molecules and NPs in augmenting the efficacy and specificity of PCR through strategic interface interactions.

The distinctive surface properties of NPs critically influence these enhancements, and their inherent high thermal conductivity significantly modulates the hydrothermal dynamics essential for optimal PCR cycling. Furthermore, the applications of photothermal and magnetothermal properties of NPs have catalyzed the development of innovative regulatory techniques, expanding the horizons of traditional PCR methodologies. Moreover, the incorporation of optical technologies into PCR protocols represents a transformative advancement. Photocaging techniques employing light-responsive molecular groups provide a robust mechanism for the remote activation and precise regulation of PCR. Notably, VSC with optical resonators has emerged as a seminal innovation, enabling meticulous control over PCR processes through sophisticated optical interactions. This method has been rigorously validated in laboratory settings, demonstrating its potential to significantly enhance the PCR performance.

The envisioned future of PCR paints a transformative picture for both clinical diagnostics and biomedical research. Looking forward, the integration of microfluidics technology, advanced optical techniques, and artificial intelligence (AI) promises to revolutionize PCR technology. First, by miniaturizing reaction chambers and manipulating fluids at the microscale, microfluidics can enable ultrafast and portable PCR platforms. This could be particularly valuable for point-of-care diagnostics in resource-limited settings. Second, techniques such as surface-enhanced Raman spectroscopy (SERS) and fluorescence resonance energy transfer (FRET) can be integrated with PCR for real-time monitoring and analysis, leading to faster and more sensitive diagnoses. Third, AI algorithms can analyze vast amounts of PCR data to identify patterns and optimize the reaction conditions for specific targets. This can significantly improve the accuracy and efficiency of the PCR assays. The convergence of technologies positions PCR as a cornerstone for personalized medicine and a powerful tool for advancing biomedical research, ultimately contributing to improved patient outcomes and groundbreaking discoveries.

These advancements are poised to transition PCR systems toward ultrafast, portable, and intelligent platforms, ideally suited for rapid, on-site diagnostics and effective disease monitoring. Such innovations are particularly vital in the context of public health crises and the advancement of precision medicine. By leveraging these cutting-edge technologies, PCR is set to become an even more indispensable tool in the biomedical sciences, offering unparalleled diagnostic and monitoring capabilities for a myriad of diseases.

AUTHOR INFORMATION

Corresponding Authors

Lihua Wang – Institute of Materiobiology, Department of Chemistry, College of Science, Shanghai University, Shanghai 200444, People's Republic of China; Email: wanglihua@shu.edu.cn

Feng Zhang – Terahertz Technology Innovation Research Institute, Terahertz Spectrum and Imaging Technology Cooperative Innovation Center, Shanghai Key Lab of Modern Optical System, University of Shanghai for Science and Technology, Shanghai 200093, People's Republic of China; Email: fzhang@usst.edu.cn

Authors

Xinmin Zhao – Terahertz Technology Innovation Research Institute, Terahertz Spectrum and Imaging Technology Cooperative Innovation Center, Shanghai Key Lab of Modern Optical System, University of Shanghai for Science and Technology, Shanghai 200093, People's Republic of China

Hongzhen Peng – Institute of Materiobiology, Department of Chemistry, College of Science, Shanghai University, Shanghai 200444, People's Republic of China

Jun Hu – Institute of Materiobiology, Department of Chemistry, College of Science, Shanghai University, Shanghai 200444, People's Republic of China

Complete contact information is available at:
<https://pubs.acs.org/10.1021/jacsau.4c00570>

Author Contributions

L.W. and F.Z.: conceptualization, funding acquisition, visualization, writing-original draft, writing-review and editing. X.Z. and H.P.: visualization, writing-original draft, writing-review and editing. J.H.: supervision, conceptualization, funding acquisition, project administration, writing-review and editing. All authors contributed to writing of the manuscript. CRediT: **Xinmin Zhao** visualization, writing-original draft, writing-review & editing; **Hongzhen Peng** visualization, writing-original draft, writing-review & editing; **Jun Hu** conceptualization, funding acquisition, project administration, supervision, writing-review & editing; **Lihua Wang** conceptualization, funding acquisition, visualization, writing-original draft, writing-review & editing; **Feng Zhang** conceptualization, funding acquisition, visualization, writing-original draft, writing-review & editing.

Funding

We are grateful to the National Natural Science Foundation of China (No. T2241002, 32271298), the National Key Research and Development Program of China (No. 2023YFB3208200), the Opening Grants of Innovation laboratory of Terahertz Biophysics (No. 23-163-00-GZ-001-001-02-01), and Wenzhou Institute of the University of Chinese Academy of Sciences (WIUCASQD2021003, WIUCASQD20210011) for support.

Notes

The authors declare no competing financial interest.

ACKNOWLEDGMENTS

We thank Prof. Jun Guo, Liping Wang, Dr. Zhouxiang Zhao, Mr. Feng Gao, Zixin Wang, Jiawei Li, and Qiankang Si for their valuable help and discussion.

REFERENCES

- (1) Mullis, K. B. The Polymerase Chain Reaction (Nobel Lecture). *Angewandte Chemie International Edition in English* **1994**, *33* (12), 1209–1213.
- (2) Mullis, K. B. Process for amplifying nucleic acid sequences. U.S. Patent 4,683,202, 1985.
- (3) Saiki, R. K.; Scharf, S.; Faloona, F.; Mullis, K. B.; Horn, G. T.; Erlich, H. A.; Arnheim, N. Enzymatic amplification of beta-globin genomic sequences and restriction site analysis for diagnosis of sickle cell anemia. *Science* **1985**, *230* (4732), 1350–1354.
- (4) Higuchi, R.; Dollinger, G.; Walsh, P. S.; Griffith, R. Simultaneous amplification and detection of specific DNA sequences. *Biotechnology (N Y)* **1992**, *10* (4), 413–417.

(5) Burgart, L. J.; Robinson, R. A.; Heller, M. J.; Wilke, W. W.; Iakobova, O. K.; Cheville, J. C. Multiplex polymerase chain reaction. *Mod. Pathol.* **1992**, *5* (3), 320–323.

(6) Saunders, N. B.; Zollinger, W. D.; Rao, V. B. A rapid and sensitive PCR strategy employed for amplification and sequencing of porA from a single colony-forming unit of *Neisseria meningitidis*. *Gene* **1993**, *137* (2), 153–162.

(7) McCullum, E. O.; Williams, B. A. R.; Zhang, J.; Chaput, J. C. Random Mutagenesis by Error-Prone PCR. *In Vitro Mutagenesis Protocols* **2010**, *634*, 103–109.

(8) Zhao, Y.; Chen, F.; Li, Q.; Wang, L.; Fan, C. Isothermal Amplification of Nucleic Acids. *Chem. Rev.* **2015**, *115* (22), 12491–12545.

(9) Nazir, I.; Zaid Mahmood, H.; E Mustafa, S. Polymerase chain reaction: a creative review. *Journal of Applied Biotechnology & Bioengineering* **2020**, *7* (4), 157–159.

(10) Desforges, J. F.; Eisenstein, B. I. The polymerase chain reaction. A new method of using molecular genetics for medical diagnosis. *N Engl J. Med.* **1990**, *322* (3), 178–183.

(11) Cao, L.; Cui, X.; Hu, J.; Li, Z.; Choi, J. R.; Yang, Q.; Lin, M.; Ying Hui, L.; Xu, F. Advances in digital polymerase chain reaction (dPCR) and its emerging biomedical applications. *Biosens Bioelectron* **2017**, *90*, 459–474.

(12) Wainman, L. M.; Sathyanarayana, S. H.; Lefferts, J. A. Applications of Digital Polymerase Chain Reaction (dPCR) in Molecular and Clinical Testing. *J. Appl. Lab Med.* **2024**, *9* (1), 124–137.

(13) Postollec, F.; Falentin, H.; Pavan, S.; Combrisson, J.; Sohier, D. Recent advances in quantitative PCR (qPCR) applications in food microbiology. *Food Microbiol* **2011**, *28* (5), 848–861.

(14) Wang, Y.; Wang, Z.; Zhang, Y.; Bai, L.; Zhao, Y.; Liu, C.; Ma, A.; Yu, H. Polymerase chain reaction-based assays for the diagnosis of human brucellosis. *Ann. Clin. Microbiol. Antimicrob* **2014**, *13* (1), 31.

(15) Artika, I. M.; Dewi, Y. P.; Nainggolan, I. M.; Siregar, J. E.; Antonjaya, U. Real-Time Polymerase Chain Reaction: Current Techniques, Applications, and Role in COVID-19 Diagnosis. *Genes (Basel)* **2022**, *13* (12), 2387.

(16) Review: Zhang, Y.; Wang, Z.; Wang, W.; Yu, H.; Jin, M. Applications of polymerase chain reaction-based methods for the diagnosis of plague (Review). *Exp Ther Med.* **2022**, *24* (2), 511.

(17) Vajpayee, K.; Dash, H. R.; Parekh, P. B.; Shukla, R. K. PCR inhibitors and facilitators - Their role in forensic DNA analysis. *Forensic Sci. Int.* **2023**, *349*, 111773.

(18) Cao, X.; Shi, X.; Yang, W.; Zhang, X.; Fan, C.; Hu, J. Enhanced specificity and efficiency of polymerase chain reactions using poly(amidoamine) dendrimers and derivatives. *Analyst* **2009**, *134* (1), 87–92.

(19) Sairkar, P.; Chouhan, S.; Batav, N.; Sharma, R. Optimization of DNA isolation process and enhancement of RAPD PCR for low quality genomic DNA of *Terminalia arjuna*. *Journal of Genetic Engineering and Biotechnology* **2013**, *11* (1), 17–24.

(20) Iakobashvili, R.; Lapidot, A. Low temperature cycled PCR protocol for Klenow fragment of DNA polymerase I in the presence of proline. *Nucleic Acids Res.* **1999**, *27* (6), 1566–1568.

(21) Sakhabutdinova, A. R.; Chemeris, A. V.; Garafutdinov, R. R. Enhancement of PCR efficiency using mono- and disaccharides. *Anal. Biochem.* **2020**, *606*, 113858.

(22) Mok, E.; Wee, E.; Wang, Y.; Trau, M. Comprehensive evaluation of molecular enhancers of the isothermal exponential amplification reaction. *Sci. Rep.* **2016**, *6* (1), 37837.

(23) Hardjasa, A.; Ling, M.; Ma, K.; Yu, H. Investigating the Effects of DMSO on PCR Fidelity Using a Restriction Digest-Based Method. *Journal of Experimental Microbiology and Immunology* **2010**, *14*, 161–164.

(24) Henke, W.; Herdel, K.; Jung, K.; Schnorr, D.; Loening, S. A. Betaine improves the PCR amplification of GC-rich DNA sequences. *Nucleic Acids Res.* **1997**, *25* (19), 3957–3958.

(25) Musso, M.; Boccardi, R.; Parodi, S.; Ravazzolo, R.; Ceccherini, I. Betaine, dimethyl sulfoxide, and 7-deaza-dGTP, a powerful mixture

- for amplification of GC-rich DNA sequences. *J. Mol. Diagn* **2006**, *8* (5), 544–550.
- (26) Bachmann, B.; Luke, W.; Hunsmann, G. Improvement of PCR amplified DNA sequencing with the aid of detergents. *Nucleic Acids Res.* **1990**, *18* (5), 1309.
- (27) Zhang, X.; Guo, J.; Song, B.; Zhang, F. Spatiotemporal Regulation of Metal Ions in the Polymerase Chain Reaction. *ACS Omega* **2022**, *7* (37), 33530–33536.
- (28) Zhang, X.; Zhu, Z.; Liu, W.; Gao, F.; Guo, J.; Song, B.; Lee, L. P.; Zhang, F. The Selective Function of Quantum Biological Electron Transfer between DNA Bases and Metal Ions in DNA Replication. *J. Phys. Chem. Lett.* **2022**, *13* (33), 7779–7787.
- (29) Sarkar, G.; Kapelner, S.; Sommer, S. S. Formamide can dramatically improve the specificity of PCR. *Nucleic Acids Res.* **1990**, *18* (24), 7465.
- (30) Shaik, G. M.; Draberova, L.; Draber, P.; Boubelik, M.; Draber, P. Tetraalkylammonium derivatives as real-time PCR enhancers and stabilizers of the qPCR mixtures containing SYBR Green I. *Nucleic Acids Res.* **2008**, *36* (15), No. e93.
- (31) Chevet, E.; Lemaitre, G.; Katinka, M. D. Low concentrations of tetramethylammonium chloride increase yield and specificity of PCR. *Nucleic Acids Res.* **1995**, *23* (16), 3343–3344.
- (32) Kreader, C. A. Relief of amplification inhibition in PCR with bovine serum albumin or T4 gene 32 protein. *Appl. Environ. Microbiol.* **1996**, *62* (3), 1102–1106.
- (33) Rouet, P. E.; Chomette, C.; Adumeau, L.; Duguet, E.; Ravaine, S. Colloidal chemistry with patchy silica nanoparticles. *Beilstein J. Nanotechnol* **2018**, *9*, 2989–2998.
- (34) Kotov, N. A.; Feng, M. Nanoparticles and proteins: how similar are they? *Chinese Bulletin of Life Sciences* **2008**, *20* (3), 375–382.
- (35) Xin, H.; Namgung, B.; Lee, L. P. Nanoplasmonic optical antennas for life sciences and medicine. *Nature Reviews Materials* **2018**, *3* (8), 228–243.
- (36) You, M.; Li, Z.; Feng, S.; Gao, B.; Yao, C.; Hu, J.; Xu, F. Ultrafast Photonic PCR Based on Photothermal Nanomaterials. *Trends Biotechnol* **2020**, *38* (6), 637–649.
- (37) Yang, Z.; Shen, B.; Yue, L.; Miao, Y.; Hu, Y.; Ouyang, R. Application of Nanomaterials to Enhance Polymerase Chain Reaction. *Molecules* **2022**, *27* (24), 8854.
- (38) Review: Popova, V.; Dmitrienko, E.; Chubarov, A. Magnetic Nanocomposites and Imprinted Polymers for Biomedical Applications of Nucleic Acids. *Magnetochemistry* **2023**, *9* (1), 12.
- (39) Li, H.; Huang, J.; Lv, J.; An, H.; Zhang, X.; Zhang, Z.; Fan, C.; Hu, J. Nanoparticle PCR: nanogold-assisted PCR with enhanced specificity. *Angew. Chem., Int. Ed. Engl.* **2005**, *44* (32), 5100–5103.
- (40) Pan, J.; Li, H.; Cao, X.; Huang, J.; Zhang, X.; Fan, C.; Hu, J. Nanogold-assisted multi-round polymerase chain reaction (PCR). *J. Nanosci Nanotechnol* **2007**, *7* (12), 4428–4433.
- (41) Vu, B. V.; Litvinov, D.; Willson, R. C. Gold nanoparticle effects in polymerase chain reaction: favoring of smaller products by polymerase adsorption. *Anal. Chem.* **2008**, *80* (14), 5462–5467.
- (42) Mi, L.; Zhu, H.; Zhang, X.; Hu, J.; Fan, C. Mechanism of the interaction between Au nanoparticles and polymerase in nanoparticle PCR. *Chin. Sci. Bull.* **2007**, *52* (17), 2345–2349.
- (43) Mandal, S.; Hossain, M.; Muruganandan, T.; Kumar, G. S.; Chaudhuri, K. Gold nanoparticles alter Taq DNA polymerase activity during polymerase chain reaction. *RSC Adv.* **2013**, *3* (43), 20793–20799.
- (44) Bai, Y.; Cui, Y.; Paoli, G. C.; Shi, C.; Wang, D.; Shi, X. Nanoparticles Affect PCR Primarily via Surface Interactions with PCR Components: Using Amino-Modified Silica-Coated Magnetic Nanoparticles as a Main Model. *ACS Appl. Mater. Interfaces* **2015**, *7* (24), 13142–13153.
- (45) Wan, W.; Yeow, J. T. The effects of gold nanoparticles with different sizes on polymerase chain reaction efficiency. *Nanotechnology* **2009**, *20* (32), 325702.
- (46) Yang, W.; Cao, X.; Li, X. Enhanced simultaneous overlap extension-PCR by gold nanoparticles. *Nanomedicine* **2017**, *13* (7), 2263–2266.
- (47) El-Husseini, D. M.; Helmy, N. M.; Tammam, R. H. Application of gold nanoparticle-assisted PCR for equine herpesvirus 1 diagnosis in field samples. *Arch. Virol.* **2017**, *162* (8), 2297–2303.
- (48) Ye, X.; Fang, X.; Li, X.; Kong, J. Gold nanoparticle-mediated nucleic acid isothermal amplification with enhanced specificity. *Anal. Chim. Acta* **2018**, *1043*, 150–157.
- (49) Haber, A. L.; Griffiths, K. R.; Jamting, A. K.; Emslie, K. R. Addition of gold nanoparticles to real-time PCR: effect on PCR profile and SYBR Green I fluorescence. *Anal Bioanal Chem.* **2008**, *392* (5), 887–896.
- (50) Cao, X.; Shen, M.; Zhang, X.; Hu, J.; Wang, J.; Shi, X. Effect of the surface functional groups of dendrimer-entrapped gold nanoparticles on the improvement of PCR. *Electrophoresis* **2012**, *33* (16), 2598–2603.
- (51) Chen, J.; Cao, X.; Guo, R.; Shen, M.; Peng, C.; Xiao, T.; Shi, X. A highly effective polymerase chain reaction enhancer based on dendrimer-entrapped gold nanoparticles. *Analyst* **2012**, *137* (1), 223–228.
- (52) Yuan, L.; He, Y. Effect of surface charge of PDDA-protected gold nanoparticles on the specificity and efficiency of DNA polymerase chain reaction. *Analyst* **2013**, *138* (2), 539–545.
- (53) Zhang, Z.; Wang, M.; An, H. An aqueous suspension of carbon nanopowder enhances the efficiency of a polymerase chain reaction. *Nanotechnology* **2007**, *18* (35), 355706.
- (54) Wang, L.; Zhu, Y.; Jiang, Y.; Qiao, R.; Zhu, S.; Chen, W.; Xu, C. Effects of quantum dots in polymerase chain reaction. *J. Phys. Chem. B* **2009**, *113* (21), 7637–7641.
- (55) Ma, L.; He, S.; Huang, J.; Cao, L.; Yang, F.; Li, L. Maximizing specificity and yield of PCR by the quantum dot itself rather than property of the quantum dot surface. *Biochimie* **2009**, *91* (8), 969–973.
- (56) Liang, G.; Ma, C.; Zhu, Y.; Li, S.; Shao, Y.; Wang, Y.; Xiao, Z. Enhanced Specificity of Multiplex Polymerase Chain Reaction via CdTe Quantum Dots. *Nanoscale Res. Lett.* **2011**, *6* (1), 51.
- (57) Sang, F.; Yang, Y.; Wang, H.; Ju, X.; Zhang, Z. Quantum dots induce hot-start effects for Taq-based polymerase chain reaction. *Journal of Biomedical Science and Engineering* **2012**, *05* (06), 295–301.
- (58) Sang, F.; Zhang, Z.; Xu, Z.; Ju, X.; Wang, H.; Zhang, S.; Guo, C. CdTe quantum dots enhance feasibility of EvaGreen-based real-time PCR with decent amplification fidelity. *Mol. Biotechnol* **2013**, *54* (3), 969–976.
- (59) Hwang, S. H.; Im, S. G.; Hah, S. S.; Cong, V. T.; Lee, E. J.; Lee, Y. S.; Lee, G. K.; Lee, D. H.; Son, S. J. Effects of upconversion nanoparticles on polymerase chain reaction. *PLoS One* **2013**, *8* (9), No. e73408.
- (60) Park, J. Y.; Back, S. H.; Chang, S. J.; Lee, S. J.; Lee, K. G.; Park, T. J. Dopamine-assisted synthesis of carbon-coated silica for PCR enhancement. *ACS Appl. Mater. Interfaces* **2015**, *7* (28), 15633–15640.
- (61) Cao, X.; Chen, J.; Wen, S.; Peng, C.; Shen, M.; Shi, X. Effect of surface charge of polyethyleneimine-modified multiwalled carbon nanotubes on the improvement of polymerase chain reaction. *Nanoscale* **2011**, *3* (4), 1741–1747.
- (62) Yüce, M.; Uysal, E.; Budak, H. Amplification yield enhancement of short DNA templates using bulk and surface-attached amine-functionalized single-wall carbon nanotubes. *Appl. Surf. Sci.* **2015**, *349*, 147–155.
- (63) Jia, J.; Sun, L.; Hu, N.; Huang, G.; Weng, J. Graphene enhances the specificity of the polymerase chain reaction. *Small* **2012**, *8* (13), 2011–2015.
- (64) Zhu, M.; Luo, C.; Zhang, F.; Liu, F.; Zhang, J.; Guo, S. Interactions of the primers and Mg²⁺ with graphene quantum dots enhance PCR performance. *RSC Adv.* **2015**, *5* (91), 74515–74522.
- (65) Jeong, H. Y.; Baek, S. H.; Chang, S.-J.; Yang, M.; Lee, S. J.; Lee, K. G.; Park, T. J. A hybrid composite of gold and graphene oxide as a PCR enhancer. *RSC Adv.* **2015**, *5* (113), 93117–93121.
- (66) Houhoula, D.; Papaparaskevas, J.; Zatsou, K.; Nikolaras, N.; Malkawi, H. I.; Mingenot-Leclercq, M. P.; Konteles, S.; Koussisis, S.; Tsakris, A.; Charvalos, E. Magnetic nanoparticle-enhanced PCR for

the detection and identification of *Staphylococcus aureus* and *Salmonella enteritidis*. *New Microbiol* **2017**, *40* (3), 165–169.

(67) Higashi, T.; Nagaoka, Y.; Minegishi, H.; Echigo, A.; Usami, R.; Maekawa, T.; Hanajiri, T. Regulation of PCR efficiency with magnetic nanoparticles in a rotating magnetic field. *Chem. Phys. Lett.* **2011**, *506* (4–6), 239–242.

(68) Higashi, T.; Minegishi, H.; Nagaoka, Y.; Fukuda, T.; Echigo, A.; Usami, R.; Maekawa, T.; Hanajiri, T. Effects of Superparamagnetic Nanoparticle Clusters on the Polymerase Chain Reaction. *Applied Sciences* **2012**, *2* (2), 303–314.

(69) Sun, C.; Cheng, Y.; Pan, Y.; Yang, J.; Wang, X.; Xia, F. Efficient polymerase chain reaction assisted by metal-organic frameworks. *Chem. Sci.* **2020**, *11* (3), 797–802.

(70) Nie, L.; Gao, L.; Yan, X.; Wang, T. Functionalized tetrapod-like ZnO nanostructures for plasmid DNA purification, polymerase chain reaction and delivery. *Nanotechnology* **2007**, *18* (1), 015101.

(71) Narang, J.; Narang, J.; Malhotra, N.; Narang, S.; Singhal, C.; Kansal, R.; Chandel, V.; Vastan, A. V.; Pundir, C. S. Replacement of magnesium chloride with magnesium nanoparticles in polymerase chain reaction. *Protocol Exchange* **2016**, 1.

(72) Rasheed, A. K.; Siddiqui, R.; Ahmed, S. M. K.; Gabriel, S.; Jalal, M. Z.; John, A.; Khan, N. A. hBN Nanoparticle-Assisted Rapid Thermal Cycling for the Detection of *Acanthamoeba*. *Pathogens* **2020**, *9* (10), 824.

(73) Upadhyay, A.; Yang, H.; Zaman, B.; Zhang, L.; Wu, Y.; Wang, J.; Zhao, J.; Liao, C.; Han, Q. ZnO Nanolower-Based NanoPCR as an Efficient Diagnostic Tool for Quick Diagnosis of Canine Vector-Borne Pathogens. *Pathogens* **2020**, *9* (2), 122.

(74) Li, M.; Lin, Y. C.; Wu, C. C.; Liu, H. S. Enhancing the efficiency of a PCR using gold nanoparticles. *Nucleic Acids Res.* **2005**, *33* (21), No. e184.

(75) Berber, S.; Kwon, Y. K.; Tomanek, D. Unusually high thermal conductivity of carbon nanotubes. *Phys. Rev. Lett.* **2000**, *84* (20), 4613–4616.

(76) Zhang, Z.; Shen, C.; Wang, M.; Han, H.; Cao, X. Aqueous suspension of carbon nanotubes enhances the specificity of long PCR. *Biotechniques* **2008**, *44* (4), 537–538.

(77) Murshed, S. M. S.; Leong, K. C.; Yang, C. Enhanced thermal conductivity of TiO₂—water based nanofluids. *International Journal of Thermal Sciences* **2005**, *44* (4), 367–373.

(78) Abdul Khaliq, R.; Sonawane, P. J.; Sasi, B. K.; Sahu, B. S.; Pradeep, T.; Das, S. K.; Mahapatra, N. R. Enhancement in the efficiency of polymerase chain reaction by TiO₂ nanoparticles: crucial role of enhanced thermal conductivity. *Nanotechnology* **2010**, *21* (25), 255704.

(79) Abdul Khaliq, R.; Kafafy, R.; Salleh, H. M.; Faris, W. F. Enhancing the efficiency of polymerase chain reaction using graphene nanoflakes. *Nanotechnology* **2012**, *23* (45), 455106.

(80) Lin, Y.; Li, J.; Yao, J.; Liang, Y.; Zhang, J.; Zhou, Q.; Jiang, G. Mechanism of gold nanoparticle induced simultaneously increased PCR efficiency and specificity. *Chin. Sci. Bull.* **2013**, *58* (36), 4593–4601.

(81) Madadelahi, M.; Ghazimirsaeed, E.; Shamloo, A. Design and fabrication of a two-phase diamond nanoparticle aided fast PCR device. *Anal. Chim. Acta* **2019**, *1068*, 28–40.

(82) Kambli, P.; Kelkar-Mane, V. Nanosized Fe₃O₄ an efficient PCR yield enhancer-Comparative study with Au, Ag nanoparticles. *Colloids Surf. B Biointerfaces* **2016**, *141*, 546–552.

(83) Lou, X.; Zhang, Y. Mechanism studies on nanoPCR and applications of gold nanoparticles in genetic analysis. *ACS Appl. Mater. Interfaces* **2013**, *5* (13), 6276–6284.

(84) Jiang, X.; Yang, M.; Liu, J. Capping Gold Nanoparticles to Achieve a Protein-like Surface for Loop-Mediated Isothermal Amplification Acceleration and Ultrasensitive DNA Detection. *ACS Appl. Mater. Interfaces* **2022**, *14* (24), 27666–27674.

(85) Cui, D.; Tian, F.; Kong, Y.; Titushikin, I.; Gao, H. Effects of single-walled carbon nanotubes on the polymerase chain reaction. *Nanotechnology* **2004**, *15* (1), 154–157.

(86) Higashi, T.; Minegishi, H.; Echigo, A.; Nagaoka, Y.; Fukuda, T.; Usami, R.; Maekawa, T.; Hanajiri, T. Nanomaterial-assisted PCR based on thermal generation from magnetic nanoparticles under high-frequency AC magnetic fields. *Chem. Phys. Lett.* **2015**, *635*, 234–240.

(87) Li, T.-J.; Chang, C.-M.; Chang, P.-Y.; Chuang, Y.-C.; Huang, C.-C.; Su, W.-C.; Shieh, D.-B. Handheld energy-efficient magneto-optical real-time quantitative PCR device for target DNA enrichment and quantification. *NPG Asia Materials* **2016**, *8* (6), No. e277.

(88) Kadu, P.; Pandey, S.; Neekhra, S.; Kumar, R.; Gadhe, L.; Srivastava, R.; Sastry, M.; Maji, S. K. Machine-Free Polymerase Chain Reaction with Triangular Gold and Silver Nanoparticles. *J. Phys. Chem. Lett.* **2020**, *11* (24), 10489–10496.

(89) Oda, R. P.; Strausbauch, M. A.; Huhmer, A. F.; Borson, N.; Jurrens, S. R.; Craighead, J.; Wettstein, P. J.; Eckloff, B.; Kline, B.; Landers, J. P. Infrared-mediated thermocycling for ultrafast polymerase chain reaction amplification of DNA. *Anal. Chem.* **1998**, *70* (20), 4361–4368.

(90) Huhmer, A. F.; Landers, J. P. Noncontact infrared-mediated thermocycling for effective polymerase chain reaction amplification of DNA in nanoliter volumes. *Anal. Chem.* **2000**, *72* (21), 5507–5512.

(91) Kim, H.; Dixit, S.; Green, C. J.; Faris, G. W. Nanodroplet real-time PCR system with laser assisted heating. *Opt Express* **2009**, *17* (1), 218–227.

(92) Son, J. H.; Cho, B.; Hong, S.; Lee, S. H.; Hoxha, O.; Haack, A. J.; Lee, L. P. Ultrafast photonic PCR. *Light: Science & Applications* **2015**, *4* (7), No. e280.

(93) Fermer, C.; Nilsson, P.; Larhed, M. Microwave-assisted high-speed PCR. *Eur. J. Pharm. Sci.* **2003**, *18* (2), 129–132.

(94) Kim, H.; Vishniakou, S.; Faris, G. W. Petri dish PCR: laser-heated reactions in nanoliter droplet arrays. *Lab Chip* **2009**, *9* (9), 1230–1235.

(95) Li, X.; Nguyen, L. V.; Hill, K.; Ebdorff-Heidepriem, H.; Scharner, E. P.; Zhao, Y.; Zhou, X.; Zhang, Y.; Warren-Smith, S. C. All-fiber all-optical quantitative polymerase chain reaction (qPCR). *Sens Actuators B Chem.* **2020**, *323*, 128681.

(96) Edwards, W. F.; Young, D. D.; Deiters, A. The effect of microwave irradiation on DNA hybridization. *Org. Biomol Chem.* **2009**, *7* (12), 2506–2508.

(97) Frohlich, H. The extraordinary dielectric properties of biological materials and the action of enzymes. *Proc. Natl. Acad. Sci. U. S. A.* **1975**, *72* (11), 4211–4215.

(98) Alexandrov, B. S.; Gelev, V.; Bishop, A. R.; Usheva, A.; Rasmussen, K. O. DNA Breathing Dynamics in the Presence of a Terahertz Field. *Phys. Lett. A* **2010**, *374* (10), 1214.

(99) Wu, K.; Qi, C.; Zhu, Z.; Wang, C.; Song, B.; Chang, C. Terahertz Wave Accelerates DNA Unwinding: A Molecular Dynamics Simulation Study. *J. Phys. Chem. Lett.* **2020**, *11* (17), 7002–7008.

(100) Zhang, X.; Guo, J.; Zhang, F. Mid-Infrared Photons Enhance Polymerase Chain Reaction Efficiency by Strong Coupling with Vibrational DNA Molecules. *ACS Photonics* **2023**, *10* (3), 751–756.

(101) Li, N.; Zhang, F. THz-PCR Based on Resonant Coupling between Middle Infrared and DNA Carbonyl Vibrations. *ACS Appl. Mater. Interfaces* **2023**, *15* (6), 8224–8231.

(102) Zhang, Q.; Yang, L.; Wang, K.; Guo, L.; Ning, H.; Wang, S.; Gong, Y. Terahertz waves regulate the mechanical unfolding of tau pre-mRNA hairpins. *iScience* **2023**, *26* (9), 107572.

(103) Dorman, G.; Prestwich, G. D. Using photolabile ligands in drug discovery and development. *Trends Biotechnol* **2000**, *18* (2), 64–77.

(104) Deiters, A.; Lusic, H. A New Photocaging Group for Aromatic N-Heterocycles. *Synthesis* **2006**, *2006* (13), 2147–2150.

(105) Young, D. D.; Edwards, W. F.; Lusic, H.; Lively, M. O.; Deiters, A. Light-triggered polymerase chain reaction. *Chem. Commun. (Camb)* **2008**, No. 4, 462–464.

(106) Young, D. D.; Lusic, H.; Lively, M. O.; Deiters, A. Restriction enzyme-free mutagenesis via the light regulation of DNA polymerization. *Nucleic Acids Res.* **2009**, *37* (8), No. e58.

(107) Chou, C.; Young, D. D.; Deiters, A. A light-activated DNA polymerase. *Angew. Chem., Int. Ed. Engl.* **2009**, *48* (32), 5950–5953.

- (108) Li, N.; Peng, D.; Zhang, X.; Shu, Y.; Zhang, F.; Jiang, L.; Song, B. Demonstration of biophoton-driven DNA replication via gold nanoparticle-distance modulated yield oscillation. *Nano Res.* **2021**, *14* (1), 40–45.
- (109) Yang, Y.; Peng, D.; Gu, Z.; Jiang, L.; Song, B. AuNP-Modulated qPCR: An Optimized System for Detecting MIR Biophotons Released in DNA Replication. *Chemistry* **2023**, *29* (8), No. e202203513.
- (110) Hirai, K.; Hutchison, J. A.; Uji, I. H. Molecular Chemistry in Cavity Strong Coupling. *Chem. Rev.* **2023**, *123* (13), 8099–8126.
- (111) Simpkins, B. S.; Dunkelberger, A. D.; Vurgaftman, I. Control, Modulation, and Analytical Descriptions of Vibrational Strong Coupling. *Chem. Rev.* **2023**, *123* (8), 5020–5048.
- (112) Thomas, A.; Lethuillier-Karl, L.; Nagarajan, K.; Vergauwe, R. M. A.; George, J.; Chervy, T.; Shalabney, A.; Devaux, E.; Genet, C.; Moran, J.; Ebbesen, T. W. Tilting a ground-state reactivity landscape by vibrational strong coupling. *Science* **2019**, *363* (6427), 615–619.
- (113) Garcia-Vidal, F. J.; Ciuti, C.; Ebbesen, T. W. Manipulating matter by strong coupling to vacuum fields. *Science* **2021**, *373*, No. eabd0336.
- (114) Gu, K.; Si, Q.; Li, N.; Gao, F.; Wang, L.; Zhang, F. Regulation of Recombinase Polymerase Amplification by Vibrational Strong Coupling of Water. *ACS Photonics* **2023**, *10* (5), 1633–1637.
- (115) Li, T. E.; Cui, B.; Subotnik, J. E.; Nitzan, A. Molecular Polaritonics: Chemical Dynamics Under Strong Light-Matter Coupling. *Annu. Rev. Phys. Chem.* **2022**, *73*, 43–71.
- (116) Ruggenthaler, M.; Sidler, D.; Rubio, A. Understanding Polaritonic Chemistry from Ab Initio Quantum Electrodynamics. *Chem. Rev.* **2023**, *123* (19), 11191–11229.
- (117) Ribeiro, R. F.; Martinez-Martinez, L. A.; Du, M.; Campos-Gonzalez-Angulo, J.; Yuen-Zhou, J. Polariton chemistry: controlling molecular dynamics with optical cavities. *Chem. Sci.* **2018**, *9* (30), 6325–6339.
- (118) Gao, F.; Guo, J.; Si, Q.; Wang, L.; Zhang, F.; Yang, F. Modification of ATP hydrolysis by Strong Coupling with O-H Stretching Vibration. *ChemPhotoChem.* **2023**, *7* (4), No. e202200330.
- (119) Bai, J.; Wang, Z.; Zhong, C.; Hou, S.; Lian, J.; Si, Q.; Gao, F.; Zhang, F. Vibrational coupling with O-H stretching increases catalytic efficiency of sucrase in Fabry-Perot microcavity. *Biochem. Biophys. Res. Commun.* **2023**, *652*, 31–34.
- (120) Hou, S.; Gao, F.; Zhong, C.; Li, J.; Zhu, Z.; Wang, L.; Zhao, Z.; Zhang, F. Vibrational Alchemy of DNA: Exploring the Mysteries of Hybridization under Cooperative Strong Coupling with Water. *ACS Photonics* **2024**, *11* (3), 1303–1310.
- (121) Zhong, C.; Hou, S.; Zhao, X.; Bai, J.; Wang, Z.; Gao, F.; Guo, J.; Zhang, F. Driving DNA Origami Coassembling by Vibrational Strong Coupling in the Dark. *ACS Photonics* **2023**, *10* (5), 1618–1623.